Tracking Accuracy Research on FLL-Assisted PLL in Ultra-tightly Integrated Navigation System

Shenglan Wang and Yandong Wang

1 Introduction

Using the Inertial Measurement Unit (IMU) output to assist the tracking loop in the satellite navigation system is called ultra-tightly integrated navigation system, which is a hot research topic in domestic and abroad [1]. The autonomy of inertial navigation system (INS) can help Global Position System (GPS) gain better positioning accuracy in high dynamic and high noise conditions. A fundamental task of every GPS carrier loop is to synchronize with the satellite carrier signals. And the synchronization error determines the system operation efficiency.

In order to get data code for further navigation solution, the carrier loops aim to lock the captured signal [2], that is, keep synchronous with signals in frequency or phase. Therefore, carrier loops can be divided into two kinds: PLL to lock phase and FLL to lock frequency. In order to track satellite signals accurately, PLL bandwidth is narrower relatively, which leads to a poor dynamic stress tolerance. In signal-tracking performance, (N − 1)th-order FLL can be equivalent to Nth-order PLL. But FLL is subject to the high bit error ratio in data demodulation [3]. FLL-assisted PLL consists of a PLL and a FLL in a coupled mode, thus it incorporates the advantages of avoiding false locks and reducing locking time. But in high dynamic conditions, tracking ability of carrier loops is still limited [4]. The inertial navigation aid can calculate the Doppler shift in advance by cooperating satellite ephemeris. INS can help GPS reduce dynamic stress error and improve tracking accuracy in the high dynamic and high noise environments [5].

In the previous researches, ultra-tightly integrated navigation system usually use a single PLL alone to track signals. Unfortunately in high-dynamics environments, single PLL is easy to lose signal-locking and not suitable to high dynamic

S. Wang (✉) · Y. Wang
School of Automation Science and Electronic Engineering,
Beihang University, Beijing 100083, China
e-mail: wangshenglan@buaa.edu.cn

Z. Deng (ed.), *Proceedings of 2017 Chinese Intelligent Automation Conference*,
Lecture Notes in Electrical Engineering 458,
https://doi.org/10.1007/978-981-10-6445-6_38

environment [6]. Therefore, this paper proved that it is necessary to introduce the FLL-assisted PLL into ultra-tightly integrated navigation system, and it can improve the precision and reduce the error.

Our work is organized as follows: Sect. 2 analyses the carrier loop error introduced by FLL assistance and IMU assistance respectively. In Sect. 3, we designed the simulation scheme to verify our theory and the results are analyzed. Finally, the conclusions are presented in Sect. 4.

2 Theoretical Analysis of Carrier Loop Error

2.1 Noise Error Model of FLL-Assisted PLL

The closed loop structure of FLL-assisted PLL is shown $F_p(s)$ in Fig. 1. On the one side, the target phase $\theta_k(s)$ goes through the phase discriminator represented as $K_p(s)$ and the PLL filter represented as. On the other side, $\theta_k(s)$ after conversion goes through the frequency discriminator $K_f(s)$ and FLL filter $F_f(s)$. The filters' outputs are used to adjust the numerical control oscillator (NCO), whose transfer function represented as. In these processes, some errors are introduced inevitably. n_p and n_f represent the thermal noise caused by phase discriminator and frequency discriminator respectively; n_{dyn} is the phase vibration error introduced by inertial navigation assistance. The specific calculation is analyzed in the next section.

Based on the loop structure, the formula of phase-tracking error in FLL-assisted PLL is deduced as follows:

$$\begin{aligned}\Delta\theta(s) = \theta(s) - K_p(s)F_p(s)N(s)[\Delta\theta(s) + n_p] \\ - K_f(s)F_f(s)N(s)[\Delta\omega(s) + n_f]\end{aligned} \tag{1}$$

where $\Delta\omega(s)$ is the output of frequency discriminator. When the system is steady, the phase error is mainly obtained by frequency, thus $\theta(s) \approx K_f(s)F_f(s)\Delta\omega(s)$, Therefore, the phase error of FLL-assisted PLL can be obtained:

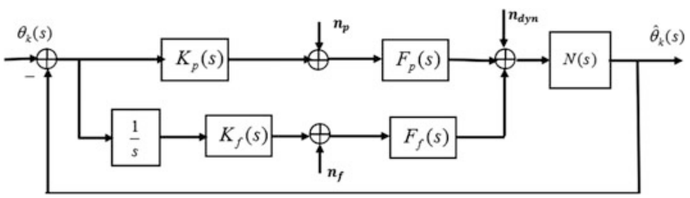

Fig. 1 Closed loop structure of FLL-assisted PLL

$$\Delta\theta(s) \approx -\frac{K_p(s)F_p(s)N(s)}{1+K_p(s)F_p(s)N(s)}n_p - \frac{K_f(s)F_f(s)N(s)}{1+K_f(s)F_f(s)N(s)}n_f \quad (2)$$

The transfer function of the PLL is defined as:

$$H_{PLL}(s) = \frac{K_p(s)F_p(s)N(s)}{1+K_p(s)F_p(s)N(s)} \quad (3)$$

The transfer function of the FLL-assisted PLL is defined as:

$$H_{FLL}(s) = [1 - H_{PLL}(s)]K_f(s)F_f(s)N(s) \quad (4)$$

Then the phase error can be written as:

$$\Delta\theta(s) \approx -H_{PLL}(s)n_p - H_{FLL}(s)n_f \quad (5)$$

2.2 Noise Error Model of Inertial Auxiliary

In the ultra-tight combination, the inertial-navigation-aid is used to estimate the Doppler shift of the current time by the IMU outputs and GPS ephemeris data. It can improve the carrier loop tracking accuracy. Feed-forward mode is used (shown in Fig. 2) which combines the INS measurement and the filter output to feed back the NCO input.

The inertial-aided noise is introduced by Doppler shift, mainly affecting phase vibration error and dynamic stress error of the carrier loop. Here the Doppler frequency auxiliary error is given as δf_d In this case, the phase tracking error with INS auxiliary is calculated as:

$$\delta\varphi(s) = [1 - H(s)] \cdot [\underset{k}{\overset{\frown}{\theta}} + \delta\varphi_d(s)] - H(s)\theta_k \quad (6)$$

where $\delta\phi_d(s) = 2\pi \cdot \delta\hat{f}_d \cdot F(s)/s$ represents the phase error introduced by Doppler shift, $F(s)$ is the inertial auxiliary transfer function, and $H(s)$ is the FLL-assisted PLL loop transfer function.

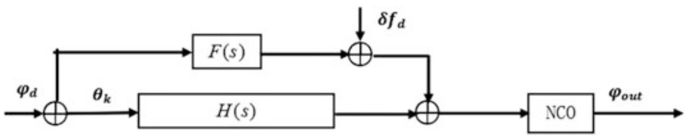

Fig. 2 A feed-forward model of INS auxiliary

According to Ref. [7], PLL phase vibration σ_d is described as follows:

$$\sigma_d^2 = \int_0^\infty |1 - H(j \cdot 2\pi f)|^2 S_d df \quad (7)$$

S_d is the first-order Markov process model of the inertial navigation auto-correlation error, written as:

$$S_d = \left(\frac{f_L}{f \cdot c}\right)^2 \left(\frac{-2\left(\frac{\ln(1-k_c)}{\Delta t}\right)\frac{k_c}{2-k_c}}{(2\pi f)^2 + \left(\frac{\ln(1-k_c)}{\Delta t}\right)^2}\right) \times 3\Delta t_{GPS} \mathrm{var}(\dot{\rho}) \quad (8)$$

where f_L is carrier frequency, Δt is the filter update time, Δt_{GPS} is the pseudo-range update time, and k_c is the filter gain. The pseudo-range error $\mathrm{var}(\dot{\rho})$ is described as:

$$\mathrm{var}(\dot{\rho}) = \left(\frac{c}{\sqrt{2}\pi f_L \Delta t_{GPS}}\right)^2 \frac{B_n}{C/N_0}\left[1 + \frac{1}{2T_{coh} \cdot C/N_0}\right] \quad (9)$$

Therefore, the FLL-assisted PLL phase vibration variance with INS auxiliary can be derived:

$$\sigma_d^2 \approx A_1^2 A_2 \mathrm{var}(\dot{\rho}) \frac{\omega_1^2 \left[\begin{array}{l} 3\omega_1^5 + 6\omega_1^2\left(\omega_1^3 + 2\sqrt{2}\omega_1^2\omega_2 + 4\omega_1\omega_2^2 + 2\sqrt{2}\omega_2^3\right) \\ + \sqrt{2}\omega_2\left(4\omega_1^4 + 2\sqrt{2}\omega_1^3\omega_2 + 5\omega_1^2\omega_2^2 + 8\sqrt{2}\omega_1\omega_2^3 + 4\omega_2^4\right) \end{array}\right]}{6\sqrt{2}\left(\begin{array}{l} \omega_1^6 + 2\sqrt{2}\omega_1^5\omega_2 + 4\omega_1^4\omega_2^2 \\ + 3\sqrt{2}\omega_1^3\omega_1^3 + 4\omega_1^2\omega_2^4 + \sqrt{2}\omega_1\omega_2^5 + \omega_2^6 \end{array}\right)} \quad (10)$$

where A_1, A_2 are considered as stationary parameters and can be described as: $A_1 = \frac{\pi f_L}{c}$; $A_2 = -\frac{6\ln(1-k_c)k_c\Delta t_{GPS}}{(2-k_c)\Delta t}$; ω_1 is the PLL angular frequency, ω_2 is the FLL angular frequency. Since the expression is too complex, we use approximate values to discuss. In previous studies [8], single PLL is used in ultra-tightly integrated navigation system, so the phase vibration error expression is only related to the PLL order, The general second-order PLL phase vibration error with inertial guidance is written as:

$$\sigma_{d,PLL}^2 = K \cdot \frac{\omega^2 + \sqrt{2}\omega + 1}{\sqrt{2}(\omega + \omega^5)} \quad (11)$$

where K is a constant factor related to carrier frequency, filter gain and i.e. In denominator, there is a ω^5 leading the phase vibration error rebounded when ω

increases. The loop bandwidth is proportional to angular frequency ω. So, using PLL alone in the ultra-tightly integrated navigation system can not reach a wide bandwidth. However, in formula (10), the maximum numerator index is larger than the maximum denominator index. Introducing FLL in ultra-tightly integrated navigation system ensures the convergence of phase vibration error.

Moreover, the dynamic stress error of the PLL is described as:

$$\sigma_{de} = \frac{1}{3} K_k \frac{d^k R/dt^k}{(B_n)^k} \cdot \frac{360 f_L}{c} \tag{12}$$

where $d^k R/dt^k$ is the relative movement in view direction between receiver and satellite, K_k is the scale factor corresponding to the kth-order PLL. This paper uses the third-order PLL and sets $K_3 = 0.4828$. In the ultra-tightly INS, the relative movement is obtained by inertial navigation and satellite ephemeris solution. In this case, the expression (12) is written as:

$$\sigma_{de} = \frac{1}{3} K_3 \frac{\delta f_{IMU}}{(B_{PLL})^k} \cdot \frac{360 f_L}{c} \tag{13}$$

where δf_{IMU} is frequency error related to IMU accuracy. The devices precision is higher, the loop dynamic stress error is smaller.

The carrier loop noise also includes the Alan variance phase noise σ_a, depending on the material and process of the receiver crystal. In this paper, σ_a is regarded as a constant value.

In summary, the FLL-assisted PLL noise variance in the ultra-tightly integrated navigation system is shown as follows:

$$\sigma = \sigma_d + \sigma_{de} + \sigma_a \tag{14}$$

3 Simulation and Results

Figure 3 illustrates the simulation for a second order FLL assisting the third order PLL in the ultra-tightly integrated navigation system:

In the figure, K_p is phase discriminator gain, K_f is frequency discriminator gain, K_0 is the NCO gain, T_s is sampling time,and f_{dyn} is Doppler shift calculated by the inertial navigation and satellite ephemeris, a_2, a_3, and b_3 are the filter parameters. ω_{n2} is the bandwidth of the second-order FLL, ω_{n3} is the bandwidth of the third-order PLL.

In order to remove High-order components due to high dynamic stress, the integrator is aim to combine the influences of different angular frequency index, and the detail structure is shown in Fig. 4.

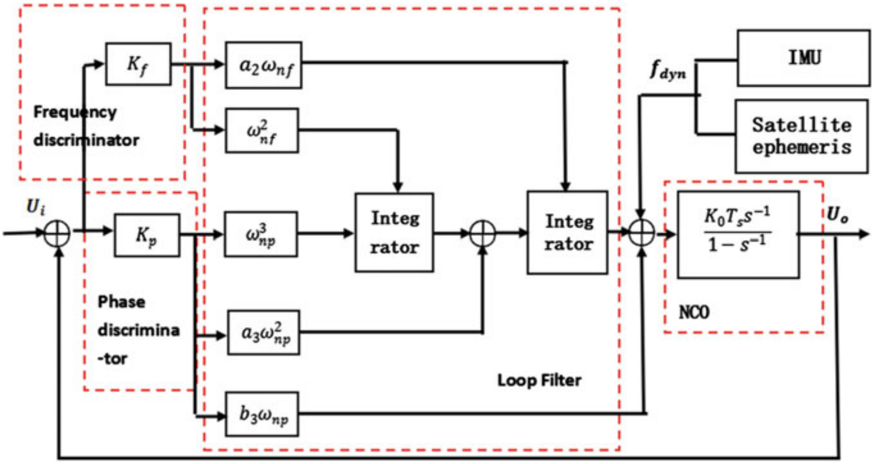

Fig. 3 The structure model of simulation

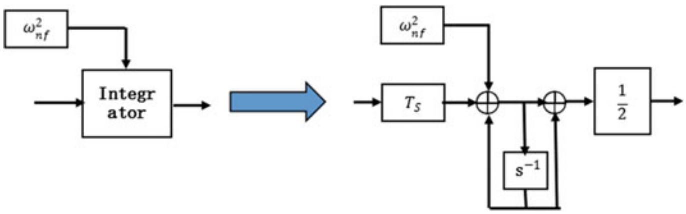

Fig. 4 Integrator structure

Simulation parameters Ref. [9], where the running time is 120 ms, the satellite intermediate frequency(IF) signal is 4.124 MHz, the phase discriminator gain is 1, the frequency discriminator gain is 0.25, and the NCO gain is 1. The filter parameters of the second-order FLL and third-order PLL picked as $a_2 = 1.414$, $a_3 = 1.1$, $b_3 = 2.4$. The bandwidth of the frequency-locked loop is $B_{L2} = 100$ Hz, angular frequency is $\omega_{n2} = \frac{B_{L2}}{0.53}$, the bandwidth of the phase-locked loop is $B_{L3} = 20$ Hz, angular frequency is $\omega_{n3} = \frac{B_{L3}}{0.7845}$, and the damping ratio is 0.707. The inertial navigation assistance transfer function is described as $F(s) = \frac{as}{s+a}$, where $a = 2\pi \times f_{dyn}$.

In order to ensure not to lose the lock of the carrier tracking loop, we select the 1σ tracking threshold 15°. Figure 5 shows the different tracking results between FLL-assisted PLL and PLL alone when they are assisted by IMU. And using FLL-assisted PLL in the ultra-tightly integrated navigation system gets better tracking accuracy.

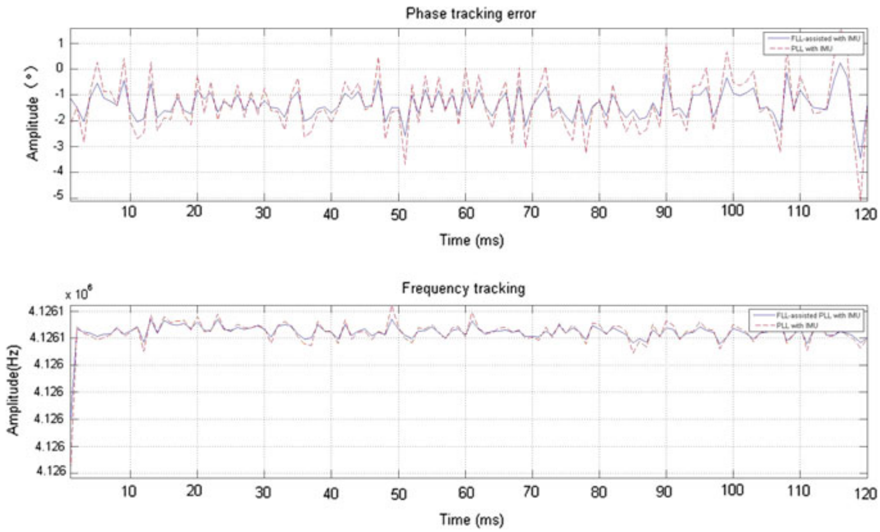

Fig. 5 Phase tracking error and frequency tracking results

Figure 6 not only compares the dynamic stress error between FLL-assisted PLL and PLL alone with IMU but also adds the FLL-assisted PLL without inertial auxiliary into comparison. However, in system without IMU assistance, the dynamic stress error is dozens times larger than that in ultra-tightly INS. Moreover, in the same system with IMU assistance, FLL-assisted PLL performs smaller dynamic stress error.

In Fig. 7, we compare the phase vibration error of FLL-assisted PLL and PLL alone in ultra-tightly integrated navigation system. In ultra-tightly INS using PLL alone, the phase vibration error rebound when the bandwidth increases to

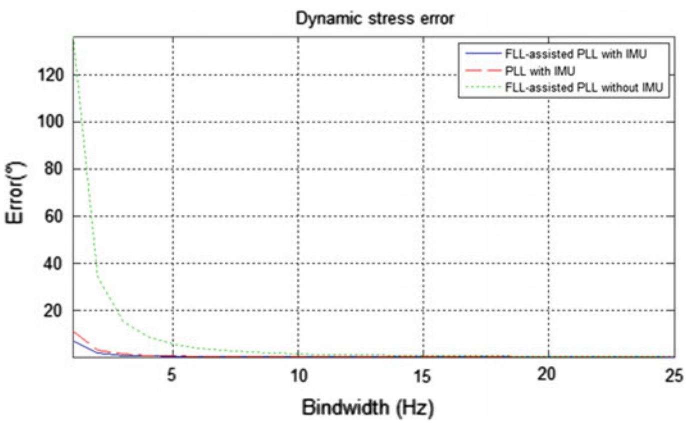

Fig. 6 Comparison of dynamic stress

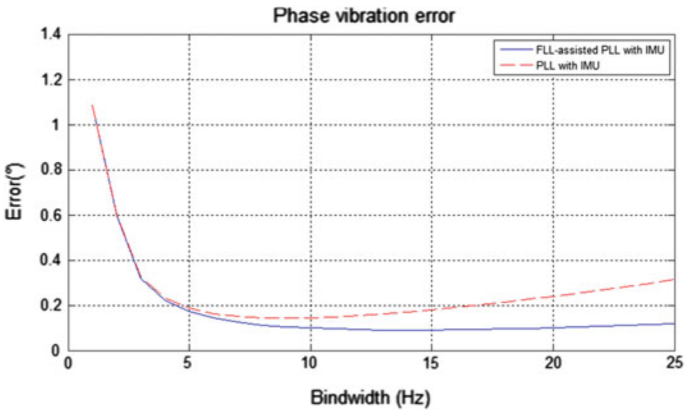

Fig. 7 Comparison of phase vibration error

approximate 15 Hz. This shortcoming is compensated by introducing the FLL assistance.

4 Conclusion

In this paper, we introduce the FLL-assisted PLL in the ultra-tightly integrated navigation system. The thermal noise and phase vibration error model are analyzed theoretically. Because of the narrow bandwidth of PLL, using PLL alone in the carrier loop can not track signals as soon as FLL. But the FLL's tracking accuracy is worse. Taking into account these two aspects, FLL-assisted PLL is a better chose in high-dynamic situations. With FLL-assisted PLL, smaller dynamic stress error and higher tracking accuracy are achieved. And it can effectively inhibit phase vibration error rebounding when the bandwidth increases to a certain extent.

References

1. Wang X, Ji X, Feng S, Calmettes V (2014) A high-sensitivity GPS receiver carrier-tracking loop design for high-dynamic applications. GPS Solut 19(2):225–236
2. Liu Y, Zhu Y (2014) A FLL-PLL cooperative GNSS weak signal tracking framework. Appl Mech Mater 551:470–477
3. Xu R, Liu Z, Chen W (2014) Improved FLL-assisted PLL with in-phase pre-filtering to mitigate amplitude scintillation effects. GPS Solut 19(2):263–276
4. Zhang T, Niu X, Ban Y, Zhang H, Shi C, Liu J (2015) Modeling and development of INS-Aided PLLs in a GNSS/INS deeply-coupled hardware prototype for dynamic applications. Sensors 15(1):733–759

5. Miura S, Kamijo S (2014) GPS error correction by multipath adaptation. Int J Intell Transp Syst Res 13(1):1–8
6. Kou Y, Zhang H (2016) Sample-wise aiding in GPS/INS ultra-tight integration for high-dynamic, high-precision tracking. Sensors 16(4):519
7. Qin F, Zhan X, Zhan L (2014) Performance assessment of a low-cost inertial measurement unit based ultra-tight global navigation satellite system/inertial navigation system integration for high dynamic applications. IET Radar Sonar Navig 8(7):828–836
8. Jiang R, Wang K, Liu S, Li Y (2016) Performance analysis of a Kalman filter carrier phase tracking loop. GPS Solutions 21(2):551–559
9. Ogaja C (2011) Applied GPS for engineers and project managers, 1st edn. ASCE, Reston